

# Automatic quality control of telemetric rain gauge data providing quantitative quality information (RainGaugeQC)

Katarzyna Ośródk<sup>1</sup>, Irena Otop<sup>2</sup>, Jan Szturc<sup>1</sup>

<sup>1</sup>Centre of Meteorological Modelling, Institute of Meteorology and Water Management – National Research Institute, PL 01-673 Warszawa, Podleśna 61, Poland

<sup>2</sup>Research and Development Centre, Institute of Meteorology and Water Management – National Research Institute, PL 01-673 Warszawa, Podleśna 61, Poland

Correspondence to: Jan Szturc (jan.szturc@imgw.pl)

**Abstract.** The RainGaugeQC scheme described in this paper is intended for real-time quality control of telemetric rain gauge data. It consists of several checks: detection of exceedance of the natural limit and climate-based threshold, and checking of the conformity of rain gauge and radar observations, the consistency of time series from heated and unheated sensors, and the spatial consistency of adjacent gauges. The proposed approach is focused on assessing the reliability of individual rain gauge observations. A quantitative indicator of reliability, called the quality index (*QI*), describes the quality of each measurement as a number in the range from 0.0 (completely unreliable measurement) to 1.0 (perfect measurement). The *QI* of a measurement which fails any check is lowered, and only a measurement very likely to be erroneous is replaced with a “no data” value. The performance of this scheme has been evaluated by analysing the spatial distribution of the precipitation field and comparing it with precipitation observations and estimates provided by other techniques. The effectiveness of the RainGaugeQC scheme was also analysed in terms of the statistics of *QI* reduction. The quality information provided is very useful in further applications of rain gauge data. The scheme is used operationally by the Polish national meteorological and hydrological service (Institute of Meteorology and Water Management – National Research Institute).

## 1 Introduction

The accuracy of telemetric rain gauge data is vital both for scientific research and for real-time modelling. Reliable precipitation measurements with high temporal and spatial resolution are essential input data for numerous operational applications in meteorology and hydrology, such as quantitative precipitation estimation (QPE), nowcasting, real-time initial conditions for numerical weather prediction, hydrological modelling, etc. Incorrect values may affect the results of these applications; this applies especially to unreasonably high or false zero precipitation values.

In recent decades, the number of automated weather station networks providing measurements with high temporal resolutions (e.g. 1-, 5-, or 10-minute) has rapidly increased. Consequently, procedures for data quality control (QC) have developed from manual or semiautomatic to fully automatic checks that provide relevant quality information, such as quality flags or quality indices (Lewis et al., 2021). However, in the case of precipitation, the effectiveness of automatic quality control methods has been proven to be much lower than in the case of other meteorological parameters (You et al., 2007). The key issue is the spatiotemporal variability of the precipitation field, which can be very intermittent and small-scale, depends strongly on the type of precipitation (e.g. convective or frontal), and also depends on topographic variables in mountainous areas with complex terrain (Scherrer et al., 2011).

This paper presents the RainGaugeQC software, which is a package of automatic QC procedures~~This paper presents the RainGaugeQC scheme with automatic QC procedures~~, developed at the Institute of Meteorology and Water Management – National Research Institute (IMGW), which operates the Polish national meteorological and hydrological service. The scheme focuses on telemetric rain gauge measurements, and is designed to identify erroneous or suspicious data and to assign a quality index (*QI*) to the individual measurements. The RainGaugeQC was designed specifically for quality control of sub-

40 [hourly rain gauge data. This is a particularly challenging task because of the higher spatial variability and lower spatial](#)  
41 [consistency of such data \(Villalobos Herrera et al., 2022\).](#)

### 42 **1.1 Sources of errors in rain gauge data**

43 Ground rain gauge measurements, like other observations, are affected by different types of errors, usually classified as  
44 random, systematic and gross errors. Random errors vary in an unpredictable manner, while systematic errors remain constant  
45 or vary in a predictable way, and can often be reduced. Gross errors are characterised by rare occurrence and large magnitude  
46 (WMO-No. 488, 2017).

47 Problems relating to the accuracy of precipitation measurement have been well documented (e.g. Sevruk, 1996; Habib  
48 et al., 2001; Golz et al., 2005; Sieck et al., 2007; Sevruk et al., 2009). The magnitude of measurement errors depends on many  
49 factors, including weather conditions at the collector, the location of the rain gauge, and the gauge type. The most significant  
50 measurement errors are related to wind (Sevruk et al., 2009; Rasmussen et al., 2012; Martinaitis et al., 2015). Wind-induced  
51 losses mainly depend on wind speed and turbulence, as well as the type of precipitation (e.g. rain, mixed snow and rain, or  
52 snow). The measurement error is usually greater for solid than for liquid precipitation (WMO-No. 8, 2018). Because of slow  
53 falling, snow hydrometers are more susceptible to deflection by wind-induced turbulence around the gauge, making snowfall  
54 measurements prone to large systematic errors (Rasmussen et al., 2012). In windy conditions, the underestimation of snowfall  
55 accumulation frequently ranges from 20% to 50% or even higher, and additionally depends on other variables, such as exposure  
56 and the type of rain gauge (Rasmussen et al., 2012; Buisán et al., 2017; Grossi et al., 2017). Other systematic error sources are  
57 related to physical processes, such as evaporation from a bucket, wetting, and splashing. All such errors are typically referred  
58 to as catching losses.

59 Additional difficulties occur in winter precipitation measurements as a result of snow collecting on the gauge or snow  
60 accumulating within wind shields, either of which can completely or partially block the gauge orifice (Goodison et al., 1998;  
61 Rasmussen et al., 2012; Martinaitis et al., 2015; Kochendorfer et al., 2020). In consequence, Martinaitis et al. (2015) identified  
62 a secondary but important impact from gauges that had become partially or completely stuck during winter precipitation events.  
63 Thawing due to increased surface ambient temperatures resulted in gauges reporting false non-zero precipitation after having  
64 collected solid precipitation. These impacts became increasingly complex when rainfall occurred simultaneously with the  
65 thawing of accumulated solid precipitation.

66 Moreover, the accuracy of precipitation measurements may be affected by improper exposure of the gauge, site altitude,  
67 shielding or obstacles (e.g. trees, buildings) near the rain gauge, the impact of topographic variables in complex areas, and the  
68 seeder–feeder effect ([when precipitation from an upper-level cloud falls through a lower-level orographic stratus cloud capping](#)  
69 [a small mountain](#)) (Førland et al., 1996; Sevruk and Nevenic, 1998).

70 Additionally, mechanical problems specific to each type of rain gauge influence the accuracy of precipitation  
71 measurements. Tipping bucket rain gauges are subject to random errors related to partial or total blockages of the mechanism  
72 due to accumulated mineral or biological particulates: dust, insects, blown grass, etc. (Sevruk, 1996; Upton and Rahimi, 2003).  
73 In consequence, even partial clogging of the gauge can result in erroneous estimates of the intensity and duration of rainfall.  
74 Another specific problem with tipping bucket rain gauges relates to high-frequency bucket tips (double tips), which lead to the  
75 recording of spurious high rainfall intensities, while on the other hand very slow tips (i.e. a limited tipping rate) may result in  
76 misleading underestimates of rain rates (Upton and Rahimi, 2003; Shedekar et al., 2016).

77 In the case of weighing gauges, the most relevant sampling errors are related to the response time of the measurement  
78 system and the consequent systematic delay in assessing the exact weight of the accumulated precipitation in the container,  
79 especially in the case of high resolution (e.g. a 1-minute time resolution). Sampling errors may also affect the measurement of  
80 low-intensity rain (Colli et al., 2013).

81 Electronic weighing precipitation gauges are less susceptible to evaporation losses than tipping bucket gauges and have  
82 better accuracy in assessing the beginning of snowfall events. A heated tipping bucket gauge starts recording with a delay due  
83 to the time needed to melt the snow and fill the first tip, and measures less precipitation due to heating-related losses (Savina  
84 et al., 2012).

85 Furthermore, precipitation measurements may be affected by gross errors, mainly caused by the malfunctioning of  
86 measurement devices, or occurring during data transmission.

## 87 1.2 Approaches to quality control of rain gauge data

88 Quality control is a vital part of data processing. ~~The World Meteorological Organisation (WMO) encourages the use of data~~  
89 ~~QC~~ in order to achieve a certain standard for international data exchange ~~(WMO No. 488, 2017)~~. The World Meteorological  
90 Organisation (WMO) ~~WMO~~ recommends initially to perform real-time basic QC of raw data at sensor level, then near-real-  
91 time QC, and finally non-real-time extended QC (semi-automatic) at the headquarters (WMO-No. 488, 2017). Performing QC  
92 at various stages of data processing makes it possible to identify the majority of errors in the dataset.

93 Generally speaking, some precipitation data QC checks consider each single observation separately (Upton and Rahimi,  
94 2003; Taylor and Loescher, 2013; Blenkinsop et al., 2017), whereas more complex ones also take into account data from  
95 neighbouring stations (Steinacker et al., 2011; Scherrer et al., 2011) or multi-source data, such as weather radar data (Yeung  
96 et al., 2014; Baserud et al., 2020) and output from a numerical weather prediction model (Qi et al., 2016). Recently, due to the  
97 increased utilisation of crowdsourced observations, specific QC methods applicable for this type of precipitation data have  
98 been developed (de Vos et al., 2019; Bárdossy et al., 2021; Niu et al., 2021).

99 For assessing the reliability of observations, several approaches are adopted. In practice, various measures of the quality  
100 of precipitation data are used. ~~They, which~~ indicate the reliability of individual sensors resulting from measurement precision,  
101 which is strongly conditioned by construction and technology (Førland et al., 1996), location, current meteorological  
102 conditions (wind, temperature), etc. Often, flags describing the quality of the data are used qualitatively; for example, the  
103 WMO recommends a scheme of five quality flags, defined as good, inconsistent, doubtful, erroneous, and missing (WMO-No.  
104 488, 2017, p. 201).

105 In the simple approach to QC outputs, the only possible result is the acceptance or rejection of particular observations.  
106 An observation that passes all of the checks is flagged as correct. If an observation fails a check, it is flagged as incorrect and  
107 does not undergo the remaining checks (Baserud et al., 2020); however, it is possible to retrieve information on which test was  
108 failed for each observation. Some QC schemes integrate the results of individual QC checks to generate a final flag for each  
109 observation. In this case an adjustment test or specially designed rule base is applied to minimise the number of correct  
110 observations that are flagged as “erroneous”. ~~F~~—for example, if an observation failed a climate-based range test but passed  
111 the spatial check, then an adjustment test may reduce the severity of the flag obtained from the climate-based range check  
112 (Fiebrich et al., 2010; Lewis et al., 2018; 2021).

113 In another approach, after failing specific checks the measured values are not removed, but corrected. Such a method  
114 may be used to replace suspicious data with values obtained from interpolation data from neighbouring stations (Michelson,  
115 2004), but it does not provide any additional information. Also, the use of data from other measurement systems is not a  
116 satisfactory solution, as these data are generally inconsistent with each other due to their different spatial distributions~~due to~~  
117 ~~the extremely different error structures~~. Generally, the correction of measured values can give unreliable results due to the high  
118 level of arbitrariness.

119 Recently, machine learning using artificial neural networks has been employed as a tool for automated quality control  
120 as well as for the correction of errors and reconstruction of missing values in precipitation data (Moslemi and Joksimovic,  
121 2018).

122 Quantitative indicators based on various forms of quality indicator can also be used, ~~describing the quality of the~~  
123 ~~observations expressed in numbers, most often~~ describing the quality of the measurement by means of a number, most often in  
124 the range from 0.0 (completely unreliable measurement) to 1.0 (perfect measurement) (Einfalt et al., 2010; Szturc et al., 2022).

125 ~~Theis latter~~ approach is adopted in the QC scheme described in this paper. In the developed RainGaugeQC scheme, the  
126 quality of uncertain measurements is lowered and only measurements very likely to be erroneous are removed – they are  
127 replaced with “no data” values. The advantage of this approach is that the quality information can be very useful in further  
128 applications. ~~E,~~ for example, it is employed in quality-based spatial interpolation of rain gauge data and in merging observations  
129 from different measurement techniques (e.g. Jurczyk et al., 2020). It seems optimal to take into account quantitative  
130 information about the quality of individual measurements in such a way that the more uncertain data are assigned a lower  
131 weight than more reliable data.

### 132 1.3 Structure of the paper

133 The paper is structured as follows. ~~After s~~Section 1, ~~provides an overview of the factors influencing the accuracy of rain gauge~~  
134 ~~measurements and the main approaches to data quality control procedures.~~ Section-section 2 briefly describes the rain gauge  
135 data on which the RainGaugeQC scheme proposed in the paper was developed and calibrated, as well as the radar data used  
136 as auxiliary data in this scheme. In section 3, the checks that constitute the RainGaugeQC system are presented (their detailed  
137 descriptions are included in the appendices). Section 4 presents and discusses specific examples of the scheme’s performance  
138 and a general analysis of its operation. The article ends with a list of conclusions resulting from the operational use of the  
139 RainGaugeQC scheme at IMGW (section 5).

## 140 2 Data sources

### 141 2.1 Rain gauge-station network in Poland

142 The Polish national meteorological and hydrological service, provided by IMGW, operates a nationwide meteorological  
143 telemetric network which consists of 503 rain gauges-stations equipped mainly with tipping bucket sensors (Fig. 1). At the  
144 synoptic stations, SEBA Hydrometrie (<https://www.seba-hydrometrie.com/>) RG-50 devices are installed, whereas ~~lower-~~  
145 levelprecipitation stations use mainly the Met One Instruments (<https://metone.com/>) 60030 and 60030H devices (unheated  
146 and heated, respectively). Telemetric precipitation measurements are available with a 10-minute time resolution: all year round  
147 for heated sensors, and in the warm part of the year – from April to October – for unheated ones.

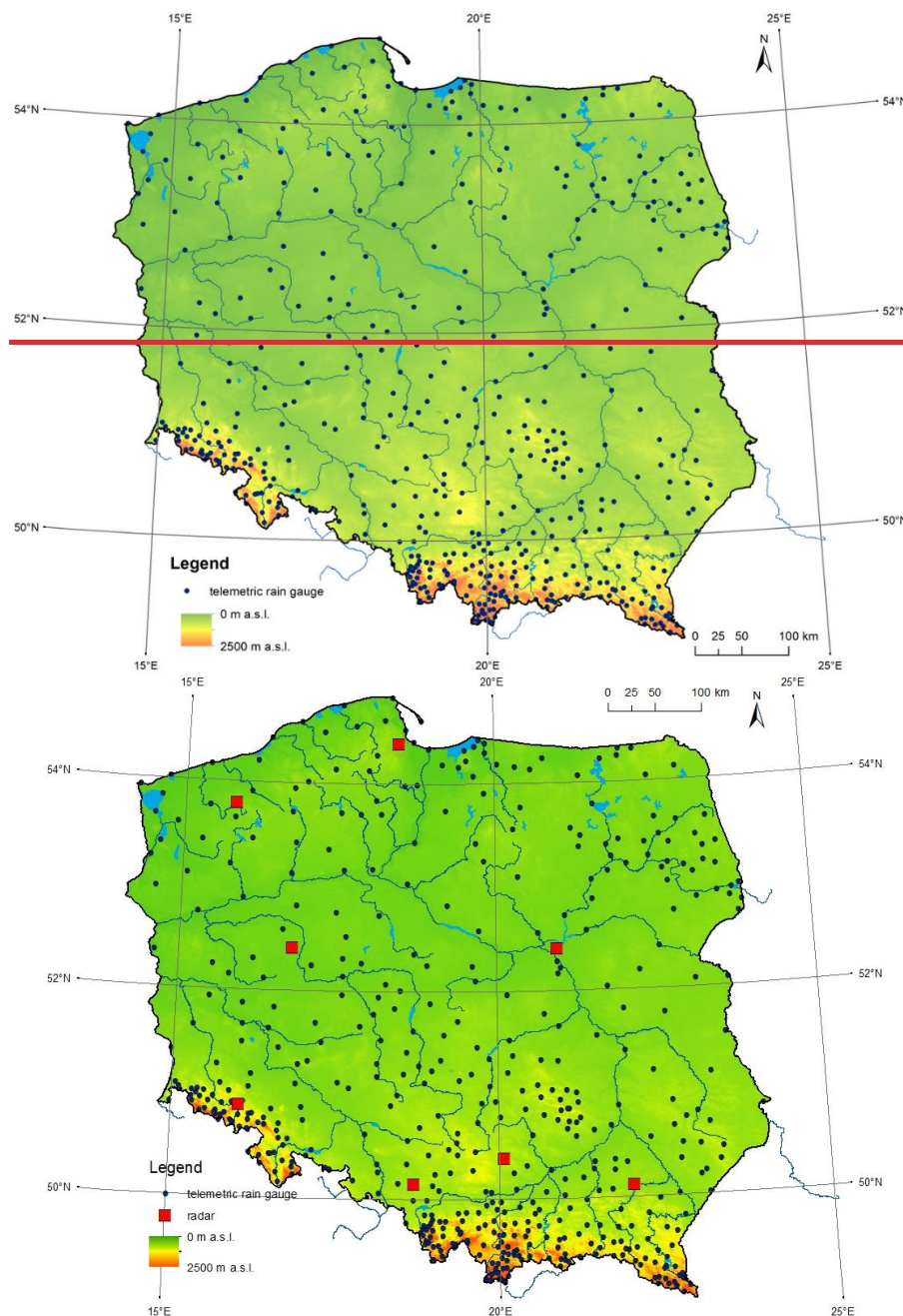


Figure 1: Networks of telemetric rain gauges stations and weather radars in Poland.

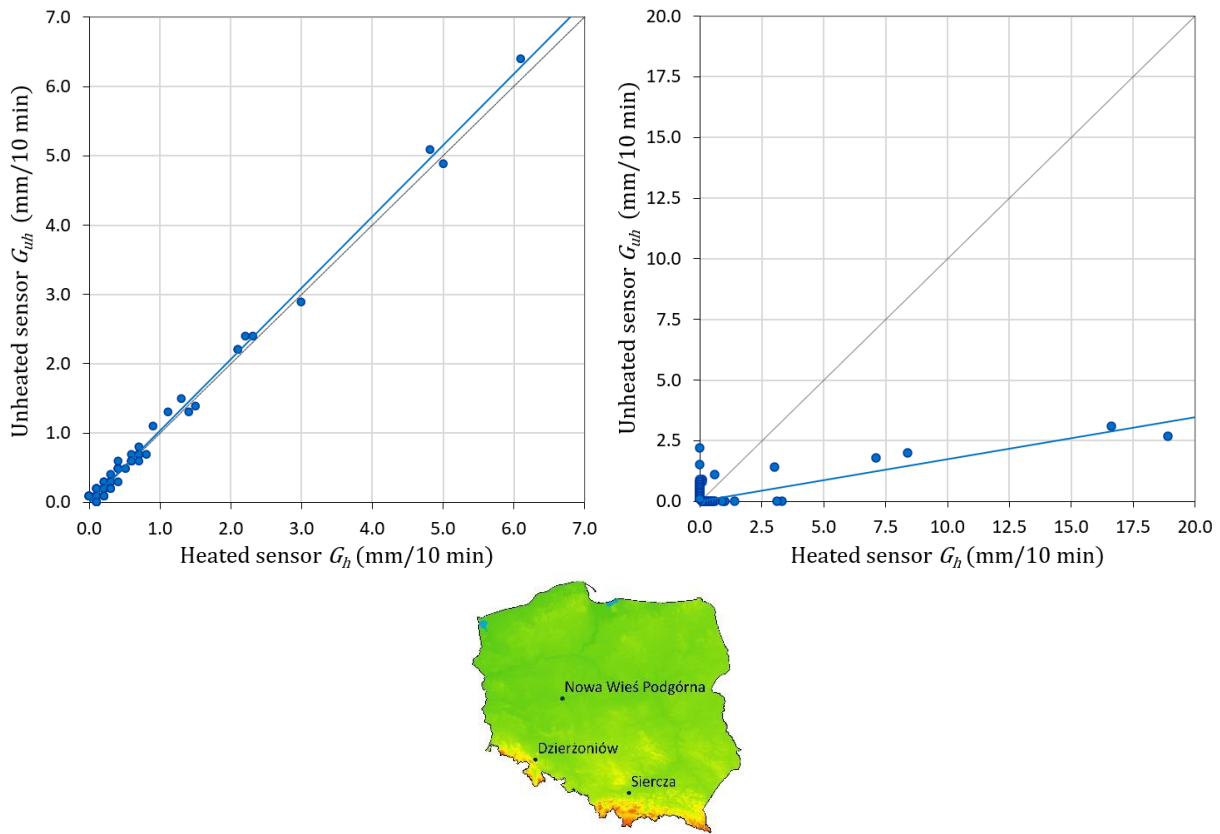
The reliability of individual rain gauges depends on the type of the gauge and its location, and changes with time. The network's tipping bucket devices often malfunction, and moreover these sensors lower the precipitation values by an average of about 8–20% (Urban and Strug, 2021).

Fig. 2 shows the relationships between measurements of 10-minute precipitation accumulations from unheated and heated sensors on two sample rain gauges stations: in Dzierżoniów, located in the foothills area, during July 2021 (left), and in Nowa Wieś Podgórna, located in the lowland Wielkopolska (Greater Poland) region in central Poland, during June 2021 (right). Both gauges stations are equipped with two tipping bucket devices sensors. The correlation coefficient calculated for pairs of values in which at least one is different from zero is extremely high for Dzierżoniów, being equal to 0.997 (Fig. 2a), while for Nowa Wieś Podgórna it is only 0.694 (Fig. 2b), a fairly low result caused by very large differences between the values measured simultaneously by the two sensors at the same location. The reason for such low correlation may be that tipping bucket gauges are susceptible to frequent sensor failures.

Generally, the left graph of Fig. 2 corresponds to a well-functioning rain gauge station, and the right graph corresponds to a rain gauge station providing data with large errors. For the latter, one or both sensors not functioning correctly recorded



166 erroneous precipitation values, and therefore they therefore require effective quality control. It is shown in section 4.3,  
167 concerning an example case study, how the quality control scheme presented in this paper worked on these obviously incorrect  
168 measurements.  
169



170  
171  
172  
173 **Figure 2: Relationships between observations of 10-minute precipitation accumulations measured with tipping bucket rain gauges**  
174 **stations** equipped with two sensors – unheated and heated – in Dzierżonów during July 2021 (left) and in Nowa Wieś Podgórna  
175 **during June 2021 (right). The blue lines mark the trends of these relationships. The data from 3 rain stations showed at the bottom**  
176 **map are discussed in the examples.**

## 177 2.2 Weather radar data

178 Weather radar data are employed in the RainGaugeQC scheme as auxiliary data to verify rain gauge observations. They are  
179 generated by the Polish radar network POLRAD, which consists of eight C-band Doppler radars from Leonardo Germany  
180 GmbH (formerly Gematronik and Selex) (Szturc et al., 2018). Three of them are dual-polarisation radars, and work is currently  
181 underway on upgrading all the radars, including dual polarization functionality~~the others will be upgraded to that functionality~~  
182 in the near future. Three- and two-dimensional radar products are generated by Rainbow 5 software every 10 min, with a 1 km  
183 spatial resolution within a 215 km range. The Marshall–Palmer formula is used to transform the reflectivity values measured  
184 by radar into the precipitation rate, this being the most common form of such a relationship (Neuper and Ehret, 2019). The  
185 data are quality controlled by the dedicated RADVOL-QC system developed at IMGW (Ośródk et al., 2014; Ośródk et al., 2022).  
186 The system also generates quality fields,  $QI(R)$ , based on analyses of particular errors disturbing radar data.

## 187 2.3. Other data

188 In addition, the fields of the following precipitation estimates were used for the case studies:

- 189 – satellite precipitation fields determined from various NWC-SAF (Satellite Application Facilities on Support to  
190 Nowcasting and Very Short Range Forecasting) products based on Meteosat data (Jurczyk et al., 2020).

- [QPE fields produced by the RainGRS system, which operationally combines precipitation data from rain gauges, weather radar and meteorological satellites, based on conditional merging and additionally taking quality information into account \(Jurczyk et al., 2020\).](#)

### 3 General description of the developed quality control scheme

#### 3.1 Set of RainGaugeQC algorithms

A shortened version of the description of the algorithms used in the scheme was presented in works by Otop et al. (2018) and Jurczyk et al. (2020). This section and the related appendices provide a full description of the developed algorithms. All parameters defined here were optimised for 10-minute precipitation accumulations (mm/10 min).

**Table 1. List of sequential checks for precipitation QC.**

ID	Abbreviation	Name	Main approach	Result of the check
1	GEC	Gross Error Check	Detection of exceedance of the natural limit	Removal of incorrect values
2	RC	Range Check	Detection of exceedance of climate-based threshold at an individual gauge	<i>QI</i> reduction for suspiciously high precipitation value
3	RCC	Radar Conformity Check	Checking of the conformity of rain gauge and radar observations	Removal of false “no precipitation” data. For false precipitation reports, <i>QI</i> reduction depending on $SF(G_h, G_{uh})$ and location
4	TCC	Temporal Consistency Check	Checking of the consistency of time series from heated and unheated sensors	<i>QI</i> reduction for inconsistent sensors
5	SCC	Spatial Consistency Check	Checking of the spatial consistency of adjacent gauges	<i>QI</i> reduction for outliers depending on the inconsistency level

The rain gauge quality control procedure developed at IMGW consists of several checks (Table 1). Firstly, simple plausibility tests – the gross error check and range check – are performed on a single measurement. ~~T~~ then more complex checks are performed, using data from both measurement sensors at the site and data from weather radars.

Before the checks, each sensor is assigned the perfect *QI* value (1.0). In case of failure of a particular check, the *QI* value is decreased by a specified value. If the final *QI* value (after all of the checks) is very weak ( $\leq 0.0$ ), the sensor is considered useless and the measurement value is replaced with “no data”.

The sensor which obtained a higher final quality index is used for further applications, but if both sensors are of the same quality, then the heated sensor is taken.

#### 3.2 Similarity function (SF)

It is useful to introduce a tool to check the similarity of two sums of precipitation. For this purpose a similarity function (*SF*) has been proposed and is used in some of the checks. The function  $SF(G_h, G_{uh})$ , comparing [precipitation](#) data from two sensors  $G_h$  and  $G_{uh}$  (heated and unheated) installed at ~~a given the same rain gauge station~~  $G$  location,  $SF(G_h, G_{uh})$ , in order to check whether the ~~precipitation-measured~~ values are consistent, is defined as follows:

If ( $G_h < 1.0$  mm or  $G_{uh} < 1.0$  mm), then

$$\text{if } (|G_h - G_{uh}| < 1.0 \text{ mm}), \text{ then } SF(G_h, G_{uh}) = \text{“true”} \quad (1)$$

$$\text{else } SF(G_h, G_{uh}) = \text{“false”}$$

whereas:

If ( $G_h \geq 1.0$  mm and  $G_{uh} \geq 1.0$  mm), then

$$\text{if } \left(0.5 < \frac{G_h}{G_{uh}} < 2.0 \text{ or } |G_h - G_{uh}| < 1.0 \text{ mm}\right), \text{ then } SF(G_h, G_{uh}) = \text{“true”} \quad (2)$$

else  $SF(G_h, G_{uh}) = \text{“false”}$

In the above formulae, precipitation units are given in “mm”, but they may refer to different accumulation periods, for example, mm per 10 minutes (mm/10 min) or 1 hour.

The result of the use of  $SF$  to assess the similarity of measurements between two sensors (heated and unheated) in rain gauges-stations is presented in Fig 3. The graph shows example data for one day, 22 May 2019, obtained from all measuring stations. It is indicated which measurements from the two sensors are shown by the  $SF$  function to be similar (marked blue) and which are not similar (marked brown). The two blue dashed lines delimit the area in which the values measured by the unheated and heated sensors are similar according to the  $SF$  function.

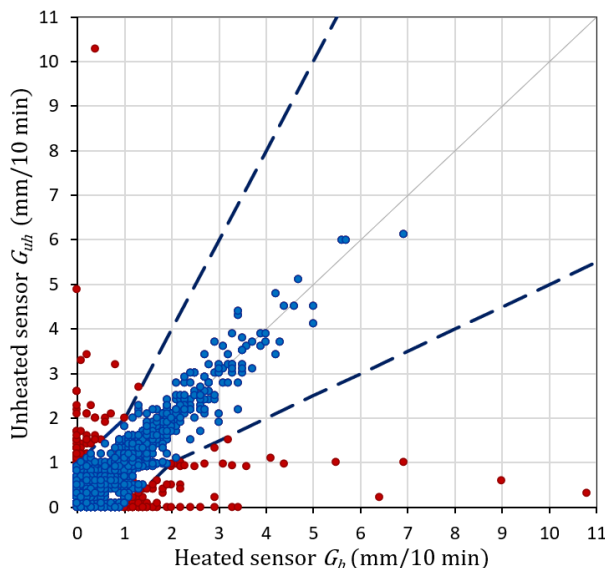


Figure 3: Precipitation data from  $G_{uh}$  and  $G_h$  sensors that are similar (blue) and not similar (brown). The similarity of the measurements from all rain gauges-stations on 22 May 2019 was determined using the similarity function  $SF$ . The two dashed lines delimit the area in which the measurements are considered similar.

### 3.3 Gross Error Check (GEC)

GEC is a preliminary check to identify gross errors which have a strong effect on the further analyses. These errors are mainly caused by the malfunctioning of measurement devices or by mistakes occurring during data transmission or processing (Steinacker et al., 2011), which have a strong effect on the further analyses. GEC examines whether the rain gauge measurement is within the physically acceptable range limits: not less than 0 mm and not above 56 mm/10 min (i.e. 51 dBZ). The upper limit was determined on the basis of a formula developed to estimate the maximum reliable precipitation for various durations in Poland (Burszta-Adamiak et al., 2019). A measurement that fails the check is rejected from further processing.

### 3.4 Range Check (RC)

RC verifies a single measurement against a threshold value, which is based on local climatological data with respect to seasonal variation of observations in the specific location of the rain gaugestation. This test identifies data as implausible when they exceed the expected maximum value, that is, the threshold empirically estimated from long-term climatological data. It is essential to ensure reliable values of the threshold, because, for example, too low a threshold may cause extreme values of precipitation to fail the test (Taylor and Loescher, 2013). Therefore, Fiebrich et al. (2010) recommend developing regionally specific thresholds for the test. In the proposed QC procedure, the thresholds were defined as 10-minute precipitation values with a 1% probability of being exceeded, determined separately for warm and cold seasons. These values were calculated for each telemetric gaugestation, based on the statistical distribution of 10-minute accumulations in a 30-year time series (1986-



251 ~~2015)over a long time.~~ In the case that the examined measurement exceeds the relevant threshold value, it is treated as  
252 suspicious and its  $QI$  is reduced by 0.25.

### 253 3.5 Radar Conformity Check (RCC)

254 RCC is performed to identify false precipitation – false zero and false gauge-reported precipitation measurements – on the  
255 basis of radar data, which quite reliably indicate the spatial distribution of precipitation. RCC compares each gauge observation  
256 lower than 0.2 mm/10 min with radar observations at the gauge location and its surrounding of 3 pixels x 3 pixels (the pixel  
257 size is 1 km x 1 km).~~RCC compares each precipitation observation lower than 0.2 mm/10 min with radar observations at the~~  
258 ~~gauge station location and in a surrounding grid of 3 pixels x 3 pixels (the pixel size is 1 km x 1 km).~~ If the radar data for the  
259 vicinity of the gauge station are above a predefined threshold, then a “no precipitation” result measured by the sensor is  
260 assumed to be false and the  $QI$  is reduced to 0.0.

261 On the other hand, the RCC compares every sensor observation  $G > 0$  mm/10 min with radar observations at the gauge  
262 location and its neighbouring of 3 pixels x 3 pixels. If the radar data is of a quality  $QI(R)$  above a predefined threshold and  
263 indicates “no precipitation” (0 mm), then the precipitation measured by the sensor is assumed to be false and the  $QI$  of that  
264 observation is reduced. The reduction depends on whether data are available from one or two sensors, on their similarity, and  
265 on the gauge location. (in mountains, foothills, or lowland areas).~~On the other hand, the RCC compares every precipitation~~  
266 ~~observation with radar observations at the gauge station location and in a neighbouring grid of 3 pixels x 3 pixels. If the radar~~  
267 ~~data indicate “no precipitation” (0 mm), with radar data quality above a predefined threshold, then the precipitation measured~~  
268 ~~by the sensor is assumed to be false and the  $QI$  of that observation is reduced. The reduction depends on whether data are~~  
269 ~~available from one or two sensors, on their similarity, and on the gauge station location (in mountains, foothills, or lowland~~  
270 ~~areas).~~ The following regions based on altitude are distinguished: lowlands (areas below 300 m a.s.l.), foothills (between 300  
271 and 600 m a.s.l.), and mountainous (areas above 600 m a.s.l.).

272 For a detailed description of the RCC algorithm and the criteria for determining the reduction of  $QI$ , see Appendix 1.

### 273 3.6 Temporal Consistency Check (TCC)

274 This check, in the form described below, is possible only when two sensors are installed at each measuring station, most often  
275 heated and unheated, as is currently the case in the IMGW network. If this is not the case, then a method commonly used in  
276 quality control of various meteorological quantities is to checking of the time continuity of the measured values. For some  
277 types of meteorological data the time consistency checks are efficient; however, in the case of precipitation data, this check  
278 would eliminate not only all questionable data but also a large amount of true data, in particular extreme values, because of  
279 the high variability of precipitation (WMO-No. 305, 1993, p. VI.21, VI.23).

280 ~~A preliminary~~The first step of this check is performed to detect a clogged sensor, which occurs if the same value is  
281 repeated over a certain period of time. In this case, the sensor’s quality is reduced to 0.0.

282 In the next step, pairs of rain gauge sensors ( $G_h, G_{uh}$ ) are tested for the existence of large differences between them.  
283 This check requires measurements from both rain gauge sensors at the same location, and can thus be conducted only in the  
284 warm half of the year, because only then two time series from the same station are available.~~half of the year.~~ In this procedure,  
285 if the number of measurement pairs is sufficient, they are accumulated and their similarity is checked using the SF function  
286 (see section 3.2). If the sums differ, the data from both sensors have failed the TCC check and their quality is reduced.

287 For a detailed description of the TCC algorithm see Appendix 2.

SCC is applied to identify outliers based on a comparison with neighbouring [gaugesstations](#). Additionally, radar data are introduced to assess the level of *QI* reduction for outliers.

There are several steps in the operational procedure for SCC. Firstly, the domain area is divided into basic subdomains with a spatial resolution of 100 km x 100 km. For each subdomain, a set of percentiles of rain gauge data and the median absolute deviation (*MAD*) are calculated.

The criterion for the spatial consistency of an individual sensor is implemented based on the index *D*, calculated using the formula of Kondragunta and Shrestha (2006). This index is compared with the threshold values defined by its set of percentiles [of the index \*D\*](#), making it possible to determine the different classes of outliers. The check is repeated for subdomains obtained by making shifts of 25 km in all four directions. If the sensor value is identified as an outlier in the basic subdomain and in the shifted subdomains, the sensor is detected as an outlier and a further procedure is applied to assess the relevant quality reduction.

For each detected outlier, two criteria are checked: (i) if data from both sensors are available for a given rain gauge and they are similar, i.e.  $SF(G_h, G_{uh}) = \text{“true”}$ , and (ii) if the data passed the TCC test. [If both criteria are met](#), then the *QI* for the sensor is not reduced. Otherwise, for additional verification, radar data in a grid of 5 [pixels](#) x 5 pixels around the gauge location are considered if they are of good quality. ~~In this case then~~ the reduction of the *QI* value depends on the class of the outlier (weak, medium, or strong) and the magnitude of the disparity with the radar data [\(the limitation imposed on the magnitude of this disparity has been determined empirically\)](#).

A detailed description of the SCC algorithm and the criteria for reduction of the *QI* value are given in Appendix 3.

The check may optionally analyse data from both sensors together or separately, and may ~~or may not~~ include [or not](#) data from the previous time step. It was investigated how these [two](#) settings influence the performance of the check.

Fig. 4 presents graphs showing the percentage of data with reduced *QI* values, as a result of analysing the spatial conformity of data from two types of sensors (unheated and heated) separately or together. The obtained sample results generally showed large variation; however, the numbers of strong outliers increased significantly (about 2.35% versus 0.6%) when the two types of sensors were analysed separately – in that case the algorithm appears much less tolerant.

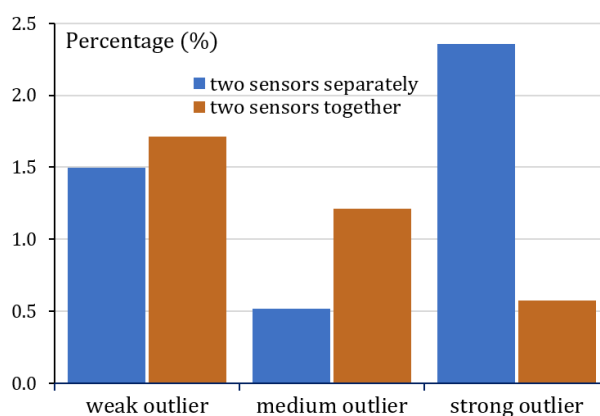
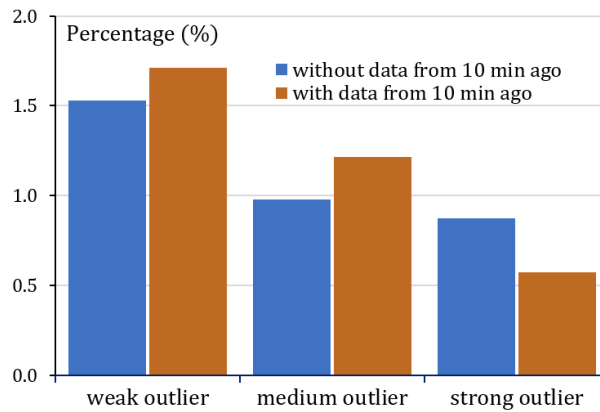


**Figure 4: Percentage of classes of outliers (weak, medium, and strong) when analysing the data from two types of sensors (unheated and heated) separately (blue) or together (brown). Data from 22 May 2019.**

If the algorithm takes into account data not only from the current time step, but also from 10 minutes ago (both sensors analysed together), then these numbers are slightly higher for weak and medium outliers and slightly lower for strong ones.

~~This observation~~ [The latter suggests](#) [indicates](#) [that the inclusion of data from the previous time step makes the algorithm more tolerant.](#) [The percentage of the data belonging to all classes of outliers together was slightly over 3%](#) ~~The percentage of the data belonging to different classes of outliers was slightly over 3%~~ (Fig. 5), [and for particular classes varies from about 1.5–](#)

323 1.7% for the weak to about 0.6–0.9% for the strong outliers and for particular classes ranged from about 1.5–1.7% for weak to  
 324 about 0.6–0.9% for strong outliers. This observation suggests that the inclusion of data from the previous time step makes the  
 325 algorithm more tolerant.



327  
 328  
 329 **Figure 5: Percentage of classes of outliers (weak, medium, and strong) when analysing measurements from the given time only (blue)**  
 330 **and also from the previous time step (brown). Data from two days: 20–21 June 2020.**

331 In the RainGaugeQC scheme currently used by IMGW in real time, in the SCC check both types of sensors are analysed  
 332 together, also taking account of the data from the previous time step.

### 333 3.8 Quality index of spatially distributed rain gauge data

334 In most applications of rain gauge data, spatial interpolation of the point data is required and this procedure can be carried out  
 335 by any of a number of, which can be performed using one of the many commonly known methods. However, it is not enough  
 336 to spatially interpolate the  $QI$  values assigned to individual rain gauges, but it is also necessary to take into account the fact  
 337 that the uncertainty of the estimated field increases very quickly with increasing distance from the nearest rain gauge due to the  
 338 natural high variability of the precipitation field, the uncertainty of the estimated field increases/decreases very quickly with  
 339 increasing distance from the nearest rain gauge. Therefore, the quality field for the spatially distributed precipitation data  
 340 depends on two factors: the  $QI$  point values for individual rain gauges (denoted by the  $QI$  with the index “ $p$ ”) and a factor that  
 341 depends linearly on the distance from the nearest rain gauge (with the index “ $d$ ”).

342 The precipitation and  $QI$  point values from rain stations are spatially interpolated simultaneously by the same method  
 343 using the same parameters, so in both cases there are the same contributions from the individual rain gauges. Hence the  
 344 obtained quality field  $QI(G_{int}(x, y))_p$  is completely consistent with precipitation field  $(G_{int}(x, y))$ . The  $QI$  point values from  
 345 rain gauges should be spatially interpolated by the same method as the precipitation field is interpolated; hence the quality  
 346 field  $QI(G_{int}(x, y))_p$  is obtained. In the case of the operational scheme used by IMGW, ordinary kriging is applied, where the  
 347 domain of 900 km x 800 km is divided into 16 subdomains of 225 km x 200 km and interpolation is performed separately in  
 348 each of them.

349 The factor related to the distance from the rain gauges  $QI(G_{int}(x, y))_d$  takes into account the decrease in the quality of  
 350 the rainfall field depending on the distance  $d(x, y)$  to the nearest rain gauge. The distance factor for each pixel is calculated  
 351 from the linear formula:

$$352 \quad QI(G_{int}(x, y))_d = \frac{d_{max} - d(x, y)}{d_{max}} \quad (3)$$

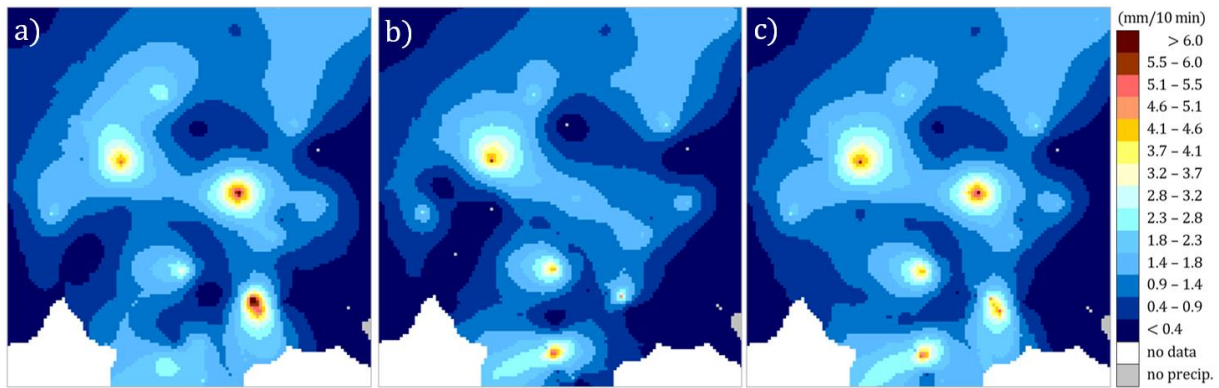
353 where  $d_{max}$  is the limit value of the distance to the nearest rain gauge, above which the quality at that pixel is assigned a value  
 354 of zero (the adopted limit is 100 km).

355 The field of the final quality index for the rain gauge-based precipitation field is calculated from the product of the two  
 356 above factors:

$$357 \quad QI(G_{\text{int}}(x, y)) = QI(G_{\text{int}}(x, y))_p \cdot QI(G_{\text{int}}(x, y))_d \quad (4)$$

## 358 4 Examples of QC scheme operation ~~for a rain gauge with low quality measurement~~

### 359 4.1 Influence of differences in values from two sensors on precipitation field estimation



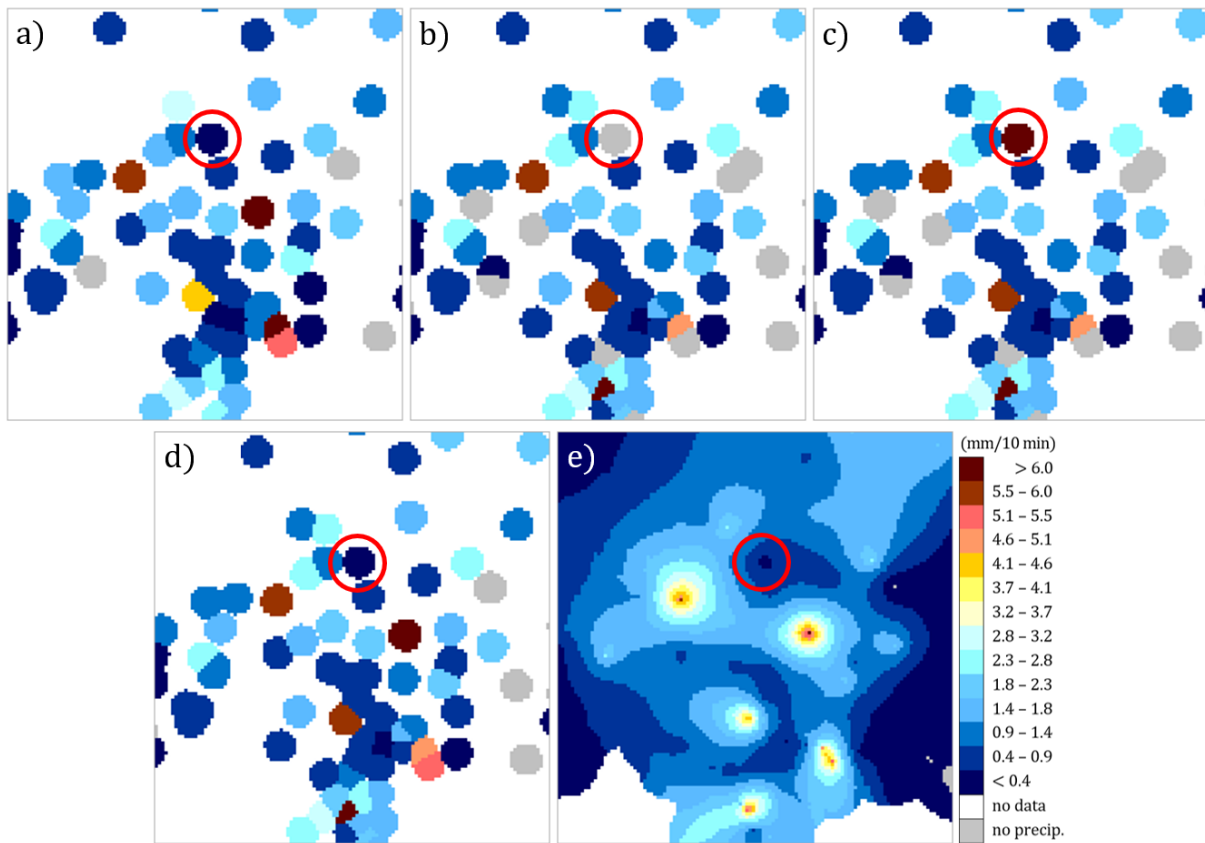
360  
 361  
 362 **Figure 6: Spatially interpolated rain gauge-station data obtained from: (a) unheated and (b) heated sensors, and (c) after quality**  
 363 **control (considered optimal). Data from 5 August 2021, 17:40 UTC, ~~excerpt-fragment~~ from the Polish domain (240 km x 250 km).**

364 In the example presented in Fig. 6, it can be seen that the data from the two sensors can sometimes be significantly different.  
 365 ~~In simpler solutions t~~The final rainfall field ~~can be generated by taking the mean or the higher values of the two sensors at the~~  
 366 ~~same location, and both of these approaches can be justified depending on the final application of the data~~~~can be simply~~  
 367 ~~generated by taking the mean or the higher values of the two sensors at the same location, and both of these approaches can~~  
 368 ~~be justified depending on the final application of the data.~~ The approach used in the RainGaugeQC scheme makes it possible  
 369 to choose the better value according to defined checks, ~~and m~~Moreover, ~~it enables to apply that precipitation value~~ along with  
 370 the relevant  $QI$  value in quality-based interpolation algorithms which generate the optimal rain gauge field.

### 371 4.2 Result of the performance of the QC scheme after the introduction of erroneous values

372 Fig. 7 illustrates the performance of the proposed QC scheme. If the rain gauge data are not subjected to QC algorithms, then  
 373 two alternative data sets can be considered: from unheated (Fig. 7a) and heated (Fig. 7b) sensors. The third diagram shows an  
 374 example of data disturbed with an artificial value of 10 mm/10 min at the heated sensor of the Siercza rain gauge-station (Fig.  
 375 7c), ~~the location of~~ which is marked with a red circle in all diagrams. ~~Location of the Siercza rain station is shown in Fig. 2~~  
 376 ~~(bottom).~~

377



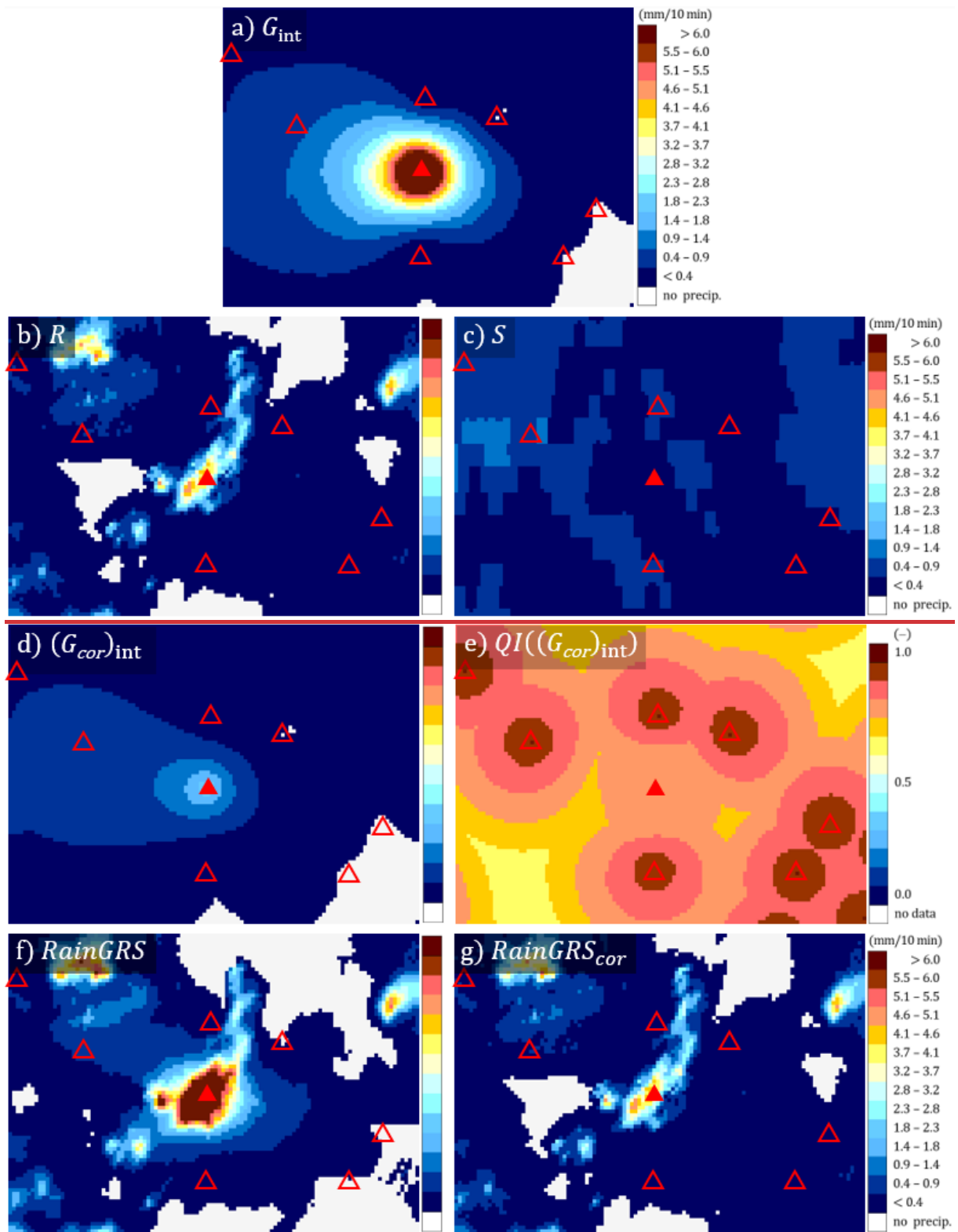
378  
379  
380 **Fig. 7. Example of the RainGaugeQC performance after the introduction of erroneous precipitation value: (a) original rain gauge**  
381 **data from unheated sensors ( $G_{uh}$ ) (in all fields the Siercza rain gauge station is marked with a red circle), (b) original data from**  
382 **heated sensors ( $G_h$ ), (c) data from heated sensors disturbed with an artificial value at Siercza (10 mm/10 min), (d) rain gauge data**  
383 **after quality control, and (e) after spatial interpolation. Data from 5 August, 2021, 17:40 UTC, excerpt-fragment from the Polish**  
384 **domain (240 km x 250 km).**

385 Fig. 7d shows the values from individual rain gauges-stations after quality control, and Fig. 7e shows the precipitation  
386 field after spatial interpolation using the ordinary kriging technique (this field is identical to the one shown in Fig. 6c). Fig. 7e  
387 shows the same values after spatial interpolation using the ordinary kriging technique (this field is identical to the one shown  
388 in Fig. 6e). As these images show, the precipitation values obtained after data quality control are some mixture of those data  
389 from both sensors that passed the QC with higher  $QI$  (see section 3.1). The Siercza rain gauge-station, marked with a red circle,  
390 serves here as an example of a gauge-station with incorrect measurement (the original values were 0.2 and 0.0 mm/10 min for  
391 unheated and heated sensors, respectively). The erroneous value of 10 mm/10 min was eliminated as a result of the QC  
392 algorithms, so the rainfall value for this rain gauge-station after QC is 0.2 mm/10 min measured by the unheated sensor.

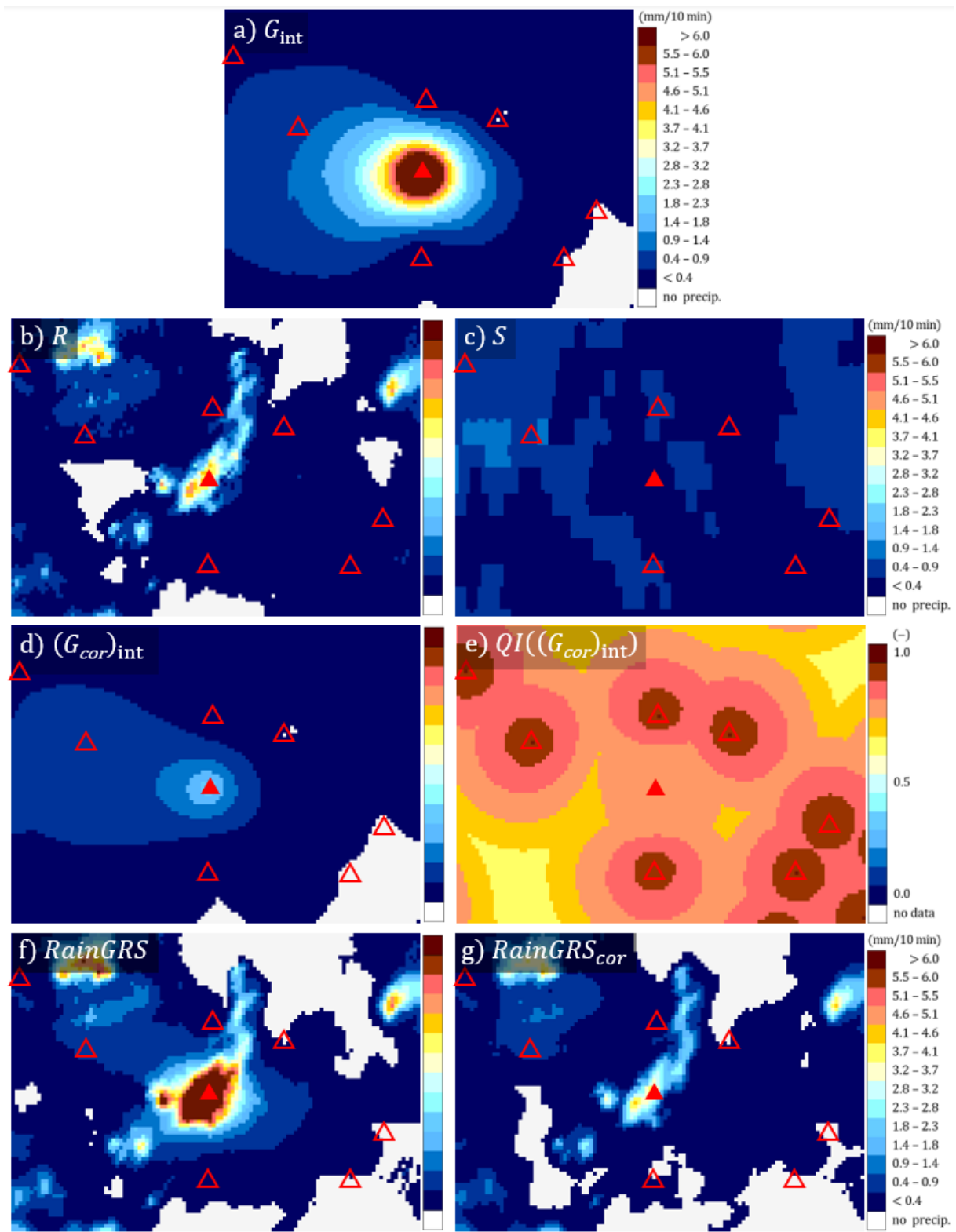
#### 393 4.3 Example for Nowa Wieś Podgórna rain gauge-station from 22 June 2021, 13:30 UTC

394 An example of a rain gauge-station with low-quality measurements, taken from the Nowa Wieś Podgórna rain gauge-station  
395 during June 2021, is shown in Fig. 2b (section 2.1). The low quality is evidenced by large differences between the values  
396 measured with heated and unheated sensors: the heated sensor recorded much higher 10-minute precipitation accumulations  
397 than the unheated one. The data from 22 June 2021, 13:30 UTC are analysed in detail below. The heated sensor of the Nowa  
398 Wieś Podgórna rain gauge-station reported a very high rainfall of 18.9 mm/10 min, whereas the unheated one reported only  
399 2.7 mm/10 min (Table 2). If QC is not performed, then the heated sensor is generally considered the primary sensor as it  
400 operates all year round. The precipitation field resulting from the interpolation of rain gauge data without QC obtained by the  
401 ordinary kriging method is shown in Fig. 8a.





403



404  
 405  
 406 **Figure 8:** Various fields of 10-minute precipitation accumulation (in mm/10 min) in the vicinity of the Nowa Wieś Podgórna rain  
 407 gauge station (marked with a red triangle; the locations of other rain gauge stations are marked with empty triangles): a) spatially  
 408 interpolated field from rain gauge data without QC ( $G_{int}$ ), b) radar-based precipitation field ( $R$ ), c) satellite-based precipitation field  
 409 ( $S$ ), d) spatially interpolated field from rain gauge data after QC ( $(G_{cor})_{int}$ ), e)  $QI$  field for the precipitation field from rain gauge  
 410 data after QC ( $QI((G_{cor})_{int})$ ), f) multi-source precipitation field ( $RainGRS$ ) obtained from raw rain gauge data, g) multi-source  
 411 precipitation field ( $RainGRS_{cor}$ ) obtained from rain gauge data after QC. Data from 22 June 2021, 13:30 UTC, excerpt-fragment  
 412 from the Polish domain (110 km x 80 km).

413 In order to diagnose the large difference between the two sensors, a detailed investigation of the situation was performed  
 414 based on precipitation data from other sources. The radar composite map from the SRI (surface rainfall intensity) product  
 415 showed 3.95 mm/10 min at this location (Fig. 8b), which is much closer to the value from the unheated sensor. Satellite rainfall,

determined from various NWC-SAF products based on Meteosat data (see Section 2.3)(Jurezyk et al., 2020), showed only 0.05 mm/10 min (Fig. 8c); however, measurements based on data from visible and infrared channels are much less accurate than radar measurements. Thus, the radar data confirmed that the rainfall that occurred in the analysed time step in the close vicinity of this rain gauge-station is significantly higher than in the surroundings, but not by as much as the heated sensor reported – it is much closer to the observation of the unheated sensor.

Visually, this conclusion seems to be unquestionable, but it may be interesting how the designed RainGaugeQC scheme functioned in this situation.

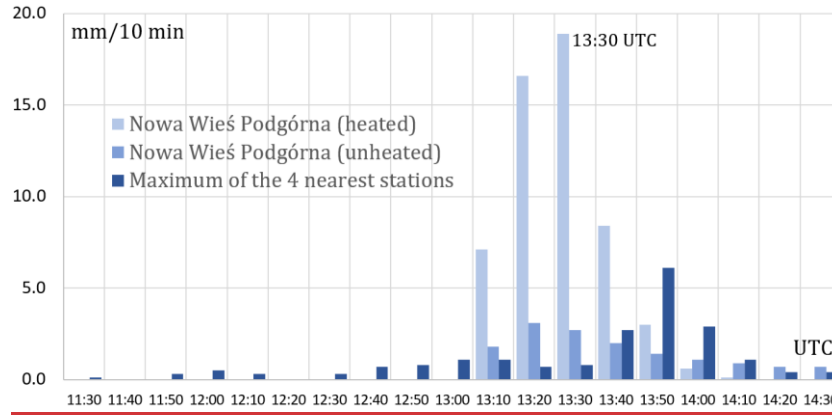


**Figure 9: Precipitation time series at Nowa Wieś Podgórna station in comparison to maximum of four neighbouring rain stations on 22 June 2021, from 11:30 to 14:30 UTC.**

Fig. 9 shows the recorded precipitation time series from 12 time steps (i.e. two hours) before the analysis date (13:30 UTC), and 6 time steps after this date, at Nowa Wieś Podgórna station (two sensors) and maximum values of the four neighbouring stations. These stations are located between 19 and 35 km from the analysed Nowa Wieś Podgórna station. Until the analysis date, precipitation measured by the sensors of these stations was not high, as it was up to about 1 mm/10 min, but 20 min later a significant increase in precipitation of about 6 mm/10 min was observed on both sensors of one of the nearby stations. At the analysed time-step only Nowa Wieś Podgórna station recorded a slightly higher precipitation on the heated sensor, while it was drastically higher on the unheated sensor (Table 2).

**Table 2. Results of QC of the Nowa Wieś Podgórna rain gauge-station on 22 June 2021, 13:30 UTC.**

Sensor	G (mm/10 min)	Check				QI (G) (-)
		RC	RSC	TCC	SCC	
Unheated	2.7	Passed	Passed	Failed	Weak outlier	0.75
Heated	18.9	Passed	Passed	Failed	Strong outlier	0.50

The quality of the data from this rain gauge-station was 0.75 for the  $G_{uh}$  sensor and 0.50 for  $G_h$ . This difference in QI values was a result of the SCC test, which showed that the  $G_{uh}$  sensor differs slightly, and the  $G_h$  sensor differs significantly, from the rainfall values in the neighbouring rain gauges-stations within the given subdomain. At the same time, both sensors failed the TCC test, which in turn indicates that the accumulated values measured by these two sensors over the last 12 time steps differ significantly (Table 2). This also contributed to a reduction in the final QI value.

Thus, finally, the value from the unheated sensor  $G_{uh}$  is taken for further processing. The precipitation field after the spatial interpolation of QC data obtained by the ordinary kriging method is shown in Fig. 8d. The precipitation values around this rain gauge-station location are clearly lower than those shown in Fig. 8a (without QC). The QI field for spatially interpolated rain gauge-datas is shown in Fig. 8e – the Nowa Wieś Podgórna rain gauge-station is of lower quality than the neighbouring rain gaugesstations.

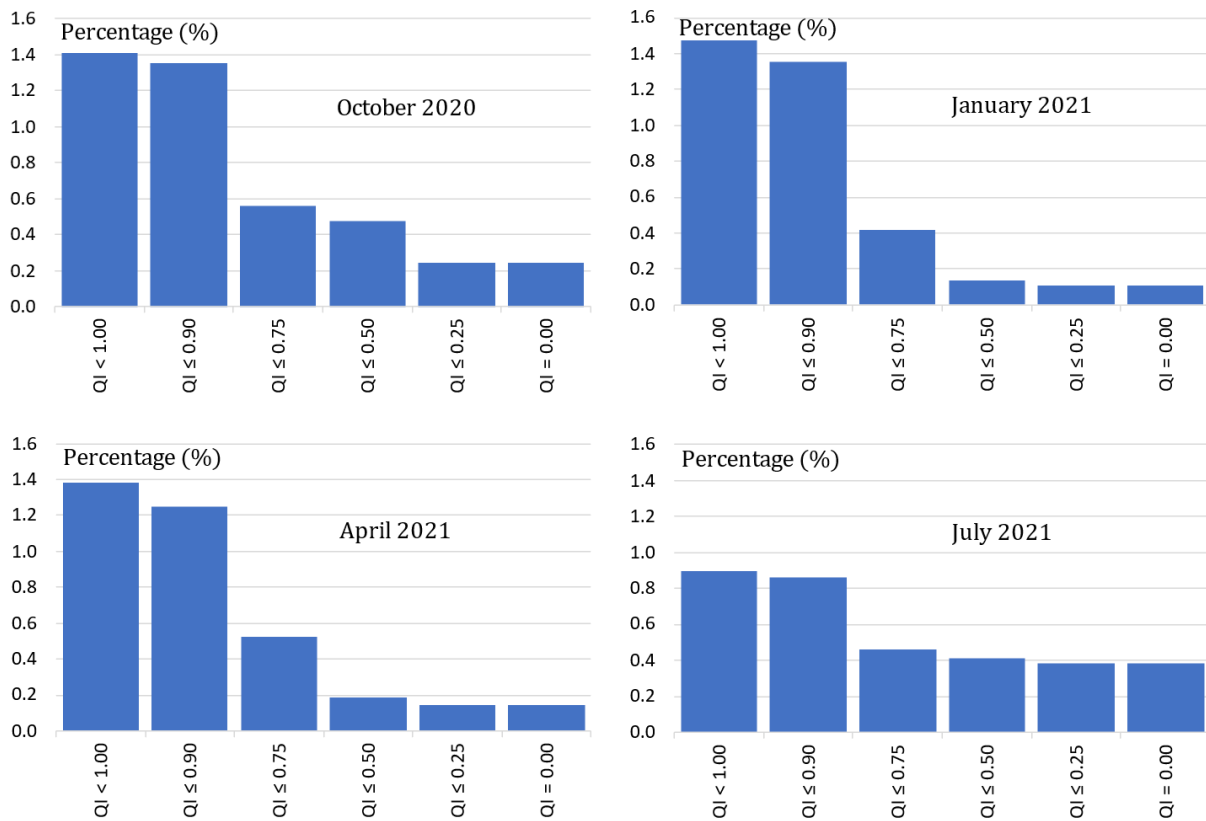
QC of rain gauge data influences the precipitation fields produced by applications for the generation of multi-source fields. This is shown by the example of the QPE fields produced by the RainGRS system, which operationally combines

449 precipitation data from rain gauges, weather radar and meteorological satellites (see Section 2.3), based on conditional merging  
 450 and additionally taking quality information into account (Jurezyk et al., 2020). In Fig. 8 two fields generated by RainGRS are  
 451 presented: based on rain gauge data without QC and after QC (Figs. 8f and 8g, respectively). Applying quality controlled rain  
 452 gauge data, the RainGRS estimate decreases from 16.19 to 3.26 mm/10 min, which is a very significant effect.

#### 453 4.4 General effects of the operation of the scheme

454 The performance of the RainGaugeQC scheme can be analysed in terms of assessed by the degree of  $QI$  reduction. This is  
 455 presented in Fig. 910, for individual months representative for autumn, winter, spring and summer conditions (October,  
 456 January, April, and July, respectively).

457



458

459

460 **Figure 910:** Percentage of rain gauge observations with a specified  $QI$  reduction after quality control. From top: percentage  
 461 contribution in each  $QI$  interval; cumulative percentage contribution (in %); from left: October 2020, January, April, and July 2021.

462

463 The graphs shown do not include the percentage contribution of measurements that were assigned a quality of 1.0; this  
 464 is equal to about ~~98.5–99.1%~~ ~~92.0–94.5%~~, many times much higher than the total contribution of all other values. In general, it  
 465 can be seen from Fig. 9-10 that by far the greatest number of reductions in  $QI$  values was to values in the range ~~([0.75, 0.90])~~,  
 466 and this is observed in all seasons of the year. Relatively large numbers of  $QI$  reductions to values in the range ~~([0.50, 0.75])~~  
 467 occur in winter (January) and spring (April), and relatively many ~~data with quality reduced to zero~~ ~~reductions to a zero~~ value  
 occur in summer (July) and autumn (October).

468

469 The number of rain gauge observations with reduced quality is relatively small, below 1.5%. For example, the  
 470 contribution of data with  $QI$  reduced to zero (i.e.  $QI = 0.0$ ) ranges from about one-third to one-tenth, but grows to about one-  
 471 half over the summer (July). In practice, this means that these data were rejected. Probably the most important reason is that  
 472 in the summer there often occurs convective precipitation, characterised by high intensities and strong spatial variability, and  
 473 moreover rain gauges in no-rain situations react to morning dew condensation, which gives false rainfall measurements  
 sometimes as high as 0.3 mm/10 min.

474 The most ~~diversified~~-diverse distribution of  $QI$  reductions is observed in winter (January): most often there are small  
475 decreases in the  $QI$  value. In summer (July), this distribution is the least varied, which can be partially explained by the  
476 numerous  $QI$  reductions to zero.

## 477 5 Conclusions

- 478 1. Quality control of rain gauge data is essential, especially from the perspective of operational applications, when it is  
479 not possible to verify gauge data employing highly reliable precipitation measurements, such as manual Hellmann  
480 rain gauges, which are not available in real time.
- 481 2. It seems that the RainGaugeQC approach to the QC of rain gauge data, which consists in estimating the value of the  
482  $QI$  of individual observations, enables more effective use of the data. On the one hand, it is a more cautious approach,  
483 as it does not eliminate all suspicious observations, and on the other hand, it enables flexible treatment of any  
484 suspected case of data incorrectness.
- 485 3. The IMGW rain gauge-station network consists mostly of rain gauges-stations equipped with two sensors: unheated  
486 and heated. This unique equipment allows the use of pairs of data to conduct much more effective QC. Comparing  
487 the observations from two sensors installed at the same location significantly increases the possibility of obtaining  
488 information about the uncertainty of measurements, for example by checking the time consistency of the data (TCC  
489 check). This is especially important when measurements are carried out with tipping bucket rain gauges, which have  
490 relatively low reliability. The availability of observations from both sensors is especially important during the warm  
491 season, when convective phenomena prevail. The frequent lack of two sensors installed at the same location reduces  
492 the scheme's effectiveness to some extent; however, it remains at a satisfactory level.
- 493 4. It is worth considering the possibility of employing radar data in the RCC and SCC algorithms to detect erroneous  
494 rain gauge measurements and to assess their reliability, based on the difference between the values from rain gauge  
495 and weather radar. The case study proved that the RainGaugeQC system can identify regionally inconsistent data  
496 thanks to the use of radar data as well as neighbouring rain gauge data.
- 497 5. The presented set of algorithms is based on empirical relationships that are strongly dependent on local conditions,  
498 both technical and geographic. The most important factors are the density of the rain gauge-station network, the  
499 availability of other data that can be used as a reference for QC (e.g. from the weather radar network), the type of  
500 sensors (their failure rate and measurement uncertainty), as well as terrain orography, wind conditions, and surface  
501 precipitation type. Therefore, any changes in the network configuration necessitate recalibration of the algorithms.
- 502 6. The number of rain gauge observations with reduced  $QI$  following QC under the RainGaugeQC scheme is relatively  
503 small, as it is below 1.5%. In all seasons, the highest number of  $QI$  value reductions was to values in the range [0.75,  
504 0.90). The highest number of erroneous data (with  $QI$  reduced to zero) is found in summer (July) (approximately  
505 0.4%), whereas in other seasons it ranges from about 0.10% to 0.23%.

## 506 Appendix 1. Detailed description of the Radar Conformity Check (RCC) algorithm

507 RCC is performed to identify false zero precipitation and false gauge-reported precipitation measurement by applying radar  
508 data.

- 509 1. Identifying false zero precipitation.

510 Each gauge sensor value ( $G$ ) less than 0.2 mm/10 min is checked against radar observations ( $R$ ) at the gauge location  
511 and in its vicinity within a grid of 3 pixels x 3 pixels.



If at least one pixel of radar data had precipitation above 0.4 mm/10 min, then the gauge value measured by this sensor is assumed to be erroneous, thus the sensor value is replaced by “no data” and the quality of this sensor is reduced to 0.

2. Identifying false gauge-reported precipitation.

Each gauge sensor value ( $G$ ) above 0 mm/10 min is checked against radar observations ( $R$ ) at the gauge location and in its vicinity within a grid of 3 pixels x 3 pixels.

If at least two radar pixels with  $QI > 0.85$  returned “no precipitation” ( $R = 0$  mm/10 min), then the following conditions are checked:

(a) If for a given rain gauge station, data are available only from one sensor ( $G$ ) and  $G > 0$  mm/10 min, then:

- if the gauge station is located in a mountain or foothill area, the sensor is considered erroneous and its value is replaced by  $G = 0$  mm and its quality reduced by 0.5;
- if the gauge station is located in a lowland area, the sensor is considered erroneous and its value is replaced by  $G = 0$  mm and its quality reduced by 0.25.

(b) If for a given rain gauge station, data are available from two sensors (heated  $G_h$  and unheated  $G_{uh}$ ) and  $G_h > 0$  mm/10 min and  $G_{uh} > 0$  mm/10 min, then:

- if the gauge station is located in a mountain or foothill area and values from both sensors are similar, i.e.  $SF(G_{uh}, G_h) = \text{“true”}$ , then the quality of both sensors is reduced by 0.75, but if  $SF(G_{uh}, G_h) = \text{“false”}$  then their qualities are reduced to  $QI = 0$  and the sensor values are replaced by “no data”;
- if the gauge station is located in a lowland area, then the sensor qualities are reduced to  $QI = 0$  and the sensor values are replaced by “no data”.

(c) If for a given rain gauge station, data are available from two sensors (heated  $G_h$  and unheated  $G_{uh}$ ) and one of them reports “no precipitation” (i.e.  $G_h = 0$  mm/10 min or  $G_{uh} = 0$  mm/10 min), then:

- if the rain gauge station is located in a mountain or foothill area and the values from both sensors are similar (i.e.  $SF(G_{uh}, G_h) = \text{“true”}$ ), then the  $QI$  of the sensor which observed precipitation  $G > 0$  mm/10 min is reduced by 0.75, but if  $SF(G_{uh}, G_h) = \text{“false”}$ , then the  $QI$  of the sensor which reports  $G > 0$  mm/10 min is reduced to  $QI = 0$  and the sensor value is replaced by “no data”;
- if the rain gauge station is located in a lowland area, then the quality of the sensor that reports  $G > 0$  mm/10 min is reduced to  $QI = 0$  and the sensor value is replaced by “no data”.

## Appendix 2. Detailed description of the Temporal Conformity Check (TCC) algorithm

~~The first step of this check is performed to detect constant values observed by a given sensor. A preliminary check is performed to detect constant values.~~ If the same value (e.g. 0.1 mm/10 min) is reported for a certain number of time steps (e.g. nine consecutive observations), then the sensor is probably clogged. In this case, the blocked sensor has failed the TCC test, its  $QI$  is reduced to 0, and the TCC test cannot be performed for the other sensor.

~~The main part of TCC serves to identify rain stations for which there are large differences between values measured simultaneously by pairs of rain sensors ( $G_h, G_{uh}$ ), which may be evidence of their low quality. The main part of TCC serves to identify pairs of rain gauge sensors ( $G_h, G_{uh}$ ) for which there are large differences between simultaneously measured values, which may be evidence of their low quality.~~ This check requires measurements from both rain gauge sensors at the same location; it can thus be conducted only in the warm season, when both sensors provide measurements. This lasts from April to October, when data from unheated sensors ( $G_{uh}$ ) are available; the heated sensors ( $G_h$ ) operate all year round.

1. Pairs of simultaneous measurements from two sensors are verified for the last 12 time steps, but observations with poor quality are not taken into account. If the number of quality-verified pairs (for previous time steps with  $QI > 0.0$ ,

and for the current one passing the previous checks, i.e. GEC, RC and RCC) is high enough (at least 9), the cumulative sums are calculated:

$$S_h = \sum_{i=1}^n G_{h,i}, \quad S_{uh} = \sum_{i=1}^n G_{uh,i} \quad (5)$$

- The similarity of the accumulated sums is checked by means of the  $SF$  function. If they differ significantly, i.e. if  $SF(S_h, S_{uh}) = \text{“false”}$ , then the data from both sensors have failed the TCC test and their quality is reduced by 0.25.

### Appendix 3. Detailed description of the Spatial Consistency Check (SCC) algorithm

The SCC procedure consists of the following steps:

- The Polish domain (900 km x 800 km) is divided into subdomains with dimensions of 100 km x 100 km. Only data with  $QI > 0$  after previous tests are subject to this check. It is optional: (i) to analyse both sensors, heated and unheated, together or separately, (ii) to include also data from the previous time step (10 min ago) if their  $QI = 1.0$ . Both sensors, heated and unheated, can be analysed together or separately, and these data can also be analysed together with data from the previous time step (10 min ago) if their  $QI = 1.0$ . In order to perform this check there must be data available from at least three stations in a subdomain, the number of data in a subdomain must be at least three; otherwise the test is not performed for that subdomain.
- Based on data from rain gauges stations ( $G$ ) located in a given subdomain, the following percentiles are determined: 25%, 50% (median), and 75% ( $Q_{25}(G)$ ,  $Q_{med}(G)$ , and  $Q_{75}(G)$ , respectively).

The median absolute deviation ( $MAD$ ) for a given subdomain is determined from the formula:

$$MAD = \frac{1}{n} \sum_{i=1}^n |G_i - Q_{med}(G)| \quad (6)$$

where  $n$  is the number of data,  $G_i$  is the  $i$ -th sensor value, and  $Q_{med}(G)$  is the median.

- The index  $D_i$ , which determines numerically the deviation of the precipitation value measured with the  $i$ -th sensor from the median of all sensors from the values of sensors within a given subdomain, is calculated from the formula (Kondragunta and Shrestha, 2006):

$$D_i = \begin{cases} 0 & MAD = 0 \\ \frac{|G_i - Q_{med}(G)|}{MAD} & MAD \neq 0 \text{ and } Q_{75}(G) = Q_{25}(G) \\ \frac{|G_i - Q_{med}(G)|}{Q_{75}(G) - Q_{25}(G)} & MAD \neq 0 \text{ and } Q_{75}(G) \neq Q_{25}(G) \end{cases} \quad (7)$$

Following calculation of the  $D_i$  values for all sensors within a given subdomain, three percentiles are determined: 90%, 95%, and 99% ( $Q_{90}(D)$ ,  $Q_{95}(D)$ , and  $Q_{99}(D)$ , respectively).

- If  $D_i \leq Q_{90}(D)$ , then the  $i$ -th sensor is not an outlier and the test is passed.

If this is not the case, the  $i$ -th sensor is flagged and the formula (8) is applied to compare the index  $D_i$  with the three percentile values, in order to determine to which class of outliers the given value belongs:

$$\text{outlier} = \begin{cases} \text{strong} & D_i > Q_{99}(D) \\ \text{medium} & Q_{95}(D) < D_i \leq Q_{99}(D) \\ \text{weak} & Q_{90}(D) < D_i \leq Q_{95}(D) \end{cases} \quad (8)$$

The procedure is repeated in four subdomains resulting from shifting the given subdomain vertically (west-east) and horizontally (south-north), i.e. in four directions, with offsets of 25 km (except for subdomains on the edges and corners of the domain, which are shifted in three and two directions, respectively). If the value measured with a given sensor is flagged in all analysed subdomains, it fails the SCC check. If the values belonged to different classes of outliers, the weakest one is assigned to the sensor for further processing.

- 587 5. For sensors that failed the SCC check, if the data from both sensors are available for a given rain gauge-station and  
588 they are similar, i.e.  $SF(G_h, G_{uh}) = \text{“true”}$ , and passed the TCC check, then the  $QI$  for the sensor is not reduced.

589 Otherwise, each outlier is verified against radar data. For this purpose the following values are determined  
590 within a grid of 5 pixels x 5 pixels around this rain gauge-station location:  $\min(QI(R))$  – the minimum quality  $QI$   
591 of the radar precipitation  $R$ ;  $R_{max} = \max(R: QI(R) > 0.75)$  – the maximum value of radar precipitation with a  
592 quality above 0.75;  $QI(R_{max})$  – the quality of the maximum value of radar precipitation  $R_{max}$ . This verification  
593 algorithm is as follows:

594 If  $\min(QI(R)) > 0.75$ , then: (9)

595 if  $R_{max} = 0$ , then the quality is reduced by 1.0 and  $G = \text{“no data”}$ ;

596 if  $(G > 1.0 \text{ mm})$  and  $\left(\frac{G}{R_{max}} < \frac{QI(R_{max})}{4.0} \text{ or } \frac{G}{R_{max}} > \frac{4.0}{QI(R_{max})}\right)$ , then:

$$597 \quad QI = \begin{cases} QI - 1.00 & \text{strong outlier} \\ QI - 0.50 & \text{medium outlier} \\ QI - 0.20 & \text{weak outlier} \end{cases}$$

598 if  $(G > 1.0 \text{ mm})$  and  $\left(\frac{G}{R_{max}} \geq \frac{QI(R_{max})}{4.0} \text{ and } \frac{G}{R_{max}} \leq \frac{4.0}{QI(R_{max})}\right)$ , then:

$$599 \quad QI = \begin{cases} QI - 0.25 & \text{strong outlier} \\ QI - 0.10 & \text{medium outlier} \\ QI & \text{weak outlier} \end{cases}$$

600 If  $(G \leq 1.0 \text{ mm})$  or  $(\min(QI(R)) \leq 0.75)$ , then:

$$601 \quad QI = \begin{cases} QI - 0.25 & \text{strong outlier} \\ QI - 0.10 & \text{medium outlier} \\ QI & \text{weak outlier} \end{cases}$$

602 where  $\frac{4.0}{QI(R_{max})}$  is the limitation to the magnitude of disparity  $\frac{G}{R_{max}}$  determined empirically.

603 An alternative simplified analysis of the spatial consistency of rain gauge data may be performed analogously to steps  
604 1–4, especially if radar data are unavailable. In this case, it is sufficient to determine only the  $Q_{95}(D)$  percentile. Here, if in all  
605 subdomains  $D_i > Q_{95}(D)$ , the sensor fails the SCC, and the QI is decreased by 0.10.~~A simpler analysis of the spatial~~  
606 ~~consistency of rain gauge data may be performed (especially if radar data are unavailable), analogously to steps 1–4, but with~~  
607 ~~only the  $Q_{95}(D)$  percentile being determined. Here, if in all subdomains  $D_i \leq Q_{95}(D)$ , the sensor fails the SCC, and the QI is~~  
608 ~~decreased by 0.10.~~

610 *Author contributions.* KO, IO, and JS designed algorithms of the RainGaugeQC system. KO developed the software code and  
611 performed the simulations. JS, IO, and KO prepared the manuscript. JS made figures.

613 *Competing interests.* The authors declare that they have no conflict of interest.

## 614 References

615 Baserud, L., Lussana, C., Nipen, T.N., Seierstad, I.A., Oram, L., and Aspelien, T.: TITAN automatic spatial quality control of  
616 meteorological in-situ observations, *Advances in Science and Research*, 17, 153-163, [https://doi.org/10.5194/asr-17-](https://doi.org/10.5194/asr-17-153-2020)  
617 153-2020, 2020.

618 Bárdossy, A., Seidel, J., and El Hachem, A.: The use of personal weather station observation for improving precipitation  
619 estimation and interpolation, *Hydrology and Earth System Sciences*, 25, 583–601, [https://doi.org/10.5194/hess-25-583-](https://doi.org/10.5194/hess-25-583-2021)  
620 2021, 2021.

621 Blenkinsop, S., Lewis, E., Chan, S.C., and Fowler, H.J.: An hourly precipitation dataset and climatology of extremes for the  
622 UK. *International Journal of Climatology*, 37, 722–740, [doi.org/10.1002/joc.4735](https://doi.org/10.1002/joc.4735), 2017.

623 Buisán, S. T., Earle, M. E., Collado, J. L., Kochendorfer, J., Alastrué, J., Wolff, M., Smith, C. D., and López-Moreno, J. I.:  
624 Assessment of snowfall accumulation underestimation by tipping bucket gauges in the Spanish operational network,  
625 *Atmospheric Measurement Techniques*, 10, 1079–1091, <https://doi.org/10.5194/amt-10-1079-2017>, 2017.

626 Burszta-Adamiak, E., Licznar, P., and Zaleski, J.: Criteria for identifying maximum rainfall determined by the peaks-over-  
627 threshold (POT) method under the Polish Atlas of Rainfall Intensities (PANDa) project, *Meteorology Hydrology and*  
628 *Water Management*, 7, 3-13, <https://doi.org/10.26491/mhwm/93595>, 2019.

629 Colli, M., Lanza, L.G., and La Barbera P.: Performance of a weighing rain gauge under laboratory simulated time-varying  
630 reference rainfall rates, *Atmospheric Research*, 131, 3-12, <https://doi.org/10.1016/j.atmosres.2013.04.006>, 2013.

631 de Vos, L. W., Leijnse, H., Overeem, A., and Uijlenhoet, R.: Quality control for crowdsourced personal weather stations to  
632 enable operational rainfall monitoring, *Geophysical Research Letters*, 46, 8820–8829,  
633 <https://doi.org/10.1029/2019GL083731>, 2019.

634 Einfalt, T., Szturc, J., and Ośródk, K.: The quality index for radar precipitation data – a tower of Babel? *Atmos. Sci. Lett.*,  
635 11, 139-144. <https://doi.org/10.1002/asl.271>, 2010.

636 Fiebrich, C. A., Morgan, C. R., and McCombs, A. G.: Quality assurance procedures for mesoscale meteorological data. *Journal*  
637 *of Atmospheric and Oceanic Technology*, 27, 1565–1582, <https://doi.org/10.1175/2010JTECHA1433.1>, 2010.

638 Førland, E. J., Allerup, P., Dahlstrom, B., Elomaa, E., Jonsson, T., Madsen, H., Perala, H., Rissanen, P., Vedin, H., and Vejen,  
639 F.: Manual for operational correction of Nordic precipitation data. Report Nr 24/96. DNMI, Norway, pp. 66, 1996.

640 Golz, C., Einfalt, T., Gabella, M., and Germann, U.: Quality control algorithms for rainfall measurements, *Atmospheric*  
641 *Research*, 77, 247-255, <https://doi.org/10.1016/j.atmosres.2004.10.027>, 2005.

642 Goodison, B.E., Louie, P.Y.T., and Yang, D.: WMO solid precipitation measurement intercomparison: Final report, *Instrum.*  
643 *Obs. Methods Rep. 67*, World Meteorological Organization, Geneva, Switzerland. pp. 211, 1998.

644 Grossi, G., Lendvai, A., Giovanni Peretti, G., and Ranzi, R.: Snow precipitation measured by gauges: systematic error  
645 estimation and data series correction in the Central Italian Alps. *Water*, 9, 461, <https://doi.org/10.3390/w9070461>, 2017.

646 Habib, E., Krajewski, W., and Kruger, A.: Sampling errors of tipping-bucket rain gauge measurements, *Journal of Hydrologic*  
647 *Engineering*, 6, 159-166, [https://doi.org/10.1061/\(ASCE\)1084-0699\(2001\)6:2\(159\)](https://doi.org/10.1061/(ASCE)1084-0699(2001)6:2(159)), 2001.

648 Jurczyk, A., Szturc, J., Otop, I., Ośródk, K., and Struzik, P.: Quality-based combination of multi-source precipitation data,  
649 *Remote Sensing*, 12, 1709, <https://doi.org/10.3390/rs12111709>, 2020.

650 Kochendorfer, J., Earle, M. E., Hodyss, D., Reverdin, A., Roulet, Y.-A., Nitu, R., Rasmussen, R., Landolt, S., Buisan, S., and  
651 Laine, T.: Undercatch adjustments for tipping-bucket gauge measurements of solid precipitation, *Journal of*  
652 *Hydrometeorology*, 21, 1193–1205, <https://doi.org/10.1175/JHM-D-19-0256.1>, 2020.

653 Kondragunta, C. R. and Shrestha, K.: Automated real-time operational rain gauge quality-control tools in NWS Hydrologic  
654 Operations. 86<sup>th</sup> AMS Annual Meeting, Atlanta, GA, 28 January – 3 March 2006, 2006.

655 Lewis, E., Quinn, N., Blenkinsop, S., Fowler, H. J., Freer, J., Tanguy, M., Hitt, O., Coxon, G., Bates, P., and Woods, R.: A  
656 rule based quality control method for hourly rainfall data and a 1 km resolution gridded hourly rainfall dataset for Great  
657 Britain: CEH-GEAR1hr, *Journal of Hydrology*, 564, 930-943, <https://doi.org/10.1016/j.jhydrol.2018.07.034>, 2018.

658 Lewis, E., Pritchard, D., Villalobos-Herrera, R., Blenkinsop, S., McClean, F., Guerreiro, S., Schneider, U., Becker, A., Finger,  
659 P., Meyer-Christoffer, A., Rustemeier, E., and Fowler, H. J.: Quality control of a global hourly rainfall dataset,  
660 *Environmental Modelling & Software*, 144, 105169, <https://doi.org/10.1016/j.envsoft.2021.105169>, 2021.

661 Martinaitis, S. M., Cocks, S. B., Qi, B., Kaney, Y., Zhang, J., and Howard, K.: Understanding winter precipitation impacts on  
662 automated gauges within a real-time system, *Journal of Hydrometeorology*, 16, 2345-2363,  
663 <https://doi.org/10.1175/JHM-D-15-0020.1>, 2015.

664 Michelson, D.: Systematic correction of precipitation gauge observations using analyzed meteorological variables, *Journal of*  
665 *Hydrology*, 290, 161–177, <https://doi.org/10.1016/j.jhydrol.2003.10.005>, 2004.

666 Moslemi, M. and Joksimovic, D.: Real-time quality control and infilling of precipitation data using neural networks, *EPiC*  
667 *Series in Engineering (HIC 2018. 13<sup>th</sup> International Conference on Hydroinformatics)*, 3, 1457-1464,  
668 <https://doi.org/10.29007/t5k7>, 2018.

669 Neuper, M. and Ehret, U.: Quantitative precipitation estimation with weather radar using a data- and information-based  
670 approach, *Hydrology and Earth System Sciences*, 23, 3711–3733, <https://doi.org/10.5194/hess-23-3711-2019>, 2019.

671 Niu, G., Yang, P., Zheng, Y., Cai, X., and Qin, H.: Automatic quality control of crowdsourced rainfall data with multiple  
672 noises: A machine learning approach, *Water Resources Research*, 57, e2020WR029121,  
673 <https://doi.org/10.1029/2020WR029121>, 2021.

674 Ośródką, K., Szturc, J., and Jurczyk A.: Chain of data quality algorithms for 3-D single-polarization radar reflectivity  
675 (RADVOL-QC system), *Meteorological Applications*, 21, 256-270, <https://doi.org/10.1002/met.1323>, 2014.

676 Ośródką, K. and Szturc, J.: Improvement in algorithms for quality control of weather radar data (RADVOL-QC system),  
677 *Atmospheric Measurement Techniques*, 15, 261-277, <https://10.5194/amt-15-261-2022>, 2022.

678 Otop, I., Szturc, J., Ośródką, K. and Djaków, P.: Automatic quality control of telemetric rain gauge data for operational  
679 applications at IMGW-PIB, *ITM Web Conf.*, 23, 00028, <https://doi.org/10.1051/itmconf/20182300028>, 2018.

680 Qi, Y., Martinaitis, S., Zhang, J., and Cocks, S.: A real-time automated quality control of hourly rain gauge data based on  
681 multiple sensors in MRMS System, *Journal of Hydrometeorology*, 17, 1675-1691, <https://doi.org/10.1175/JHM-D-15-0188.1>, 2016.

683 Rasmussen, R., Baker, B., Kochendorfer, J., Meyers, T., Landolt, S., Fischer, A. P., Black, J., Theriault, J. M., Kucera, P.,  
684 Gochis, D., Smith, C., Nitu, R., Hall, M., Ikeda, K., and Gutmann, E.: How well are we measuring snow? The  
685 NOAA/FAA/NCAR winter precipitation Test Bed, *Bulletin of the American Meteorological Society*, 93, 811-829,  
686 <https://doi.org/10.1175/BAMS-D-11-00052.1>, 2012.

687 Savina, M., Schappi, B., Molnar, P., Burlando, P., and Sevruc, B.: Comparison of a tipping-bucket and electronic weighing  
688 precipitation gauge for snowfall, *Atmospheric Research*, 103, 54-51, <https://doi.org/10.1016/j.atmosres.2011.06.010>,  
689 2012.

690 Scherrer, S. C., Frei, C., Croci-Maspoli, M., van Geijtenbeek, D., Hotz, C., and Appenzeller C.: Operational quality control of  
691 daily precipitation using spatio-climatological plausibility testing, *Meteorologische Zeitschrift*, 20, 397-407,  
692 <https://doi.org/10.1127/0941-2948/2011/0236>, 2011.

693 Sevruc, B.: Adjustment of tipping-bucket precipitation gauge measurements, *Atmospheric Research*, 42, 237-246,  
694 [https://doi.org/10.1016/0169-8095\(95\)00066-6](https://doi.org/10.1016/0169-8095(95)00066-6), 1996.

695 Sevruc, B. and Nevenic, M.: The geography and topography effects on the areal pattern of precipitation in a small prealpine  
696 basin, *Water Science and Technology*, 37, 163-170, 1998.

697 Sevruc, B., Ondras M., and Chvila B.: The WMO precipitation intercomparisons, *Atmospheric Research*, 92, 376-380,  
698 <https://doi.org/10.1016/j.atmosres.2009.01.016>, 2009.

699 Shedekar, V. S., King, K. W., Fausey, N. R., Soboyejo, A. B. O., Harmel, R. D., and Brown, L. C.: Assessment of measurement  
700 errors and dynamic calibration methods for three different tipping bucket rain gauges, *Atmospheric Research*, 178, 445-  
701 458, <https://doi.org/10.1016/j.atmosres.2016.04.016>, 2016.

702 Sieck, L.C., Burges, S. J. and Steiner, M.: Challenges in obtaining reliable measurements of point rainfall, *Water Resources*  
703 *Research*, 43, W01420, <https://doi.org/10.1029/2005WR004519>, 2007.



704 Steinacker, R., Mayer, D., Steiner, A.: Data quality control based on self-consistency, *Monthly Weather Review*, 139, 3974–  
705 3991, <https://doi.org/10.1175/MWR-D-10-05024.1>, 2011.

706 Szturc, J., Jurczyk, A., Ośródk, K., Wyszogrodzki, A., and Giszterowicz, M.: Precipitation estimation and nowcasting at  
707 IMGW (SEiNO system), *Meteorology Hydrology and Water Management*, 6, 3–12,  
708 <https://doi.org/10.26491/mhwm/76120>, 2018.

709 Szturc, J., Ośródk, K., Jurczyk, A., Otop, I., Linkowska, J., Bochenek, B., and Pasierb, M.: Quality control and verification  
710 of precipitation observations, estimates, and forecasts, in: *Precipitation Science. Measurement, Remote Sensing,*  
711 *Microphysics and Modeling*, Michaelides, S., edited by: Elsevier 2022, 91-133, [https://doi.org/10.1016/B978-0-12-](https://doi.org/10.1016/B978-0-12-822973-6.00002-0)  
712 [822973-6.00002-0](https://doi.org/10.1016/B978-0-12-822973-6.00002-0), 2022.

713 Taylor, J. R. and Loescher, H. L.: Automated quality control methods for sensor data: a novel observatory approach,  
714 *Biogeosciences*, 10, 4957-4971, <https://doi.org/10.5194/bg-10-4957-2013>, 2013.

715 Upton, G. and Rahimi A.: On-line detection of errors in tipping-bucket raingauges, *Journal of Hydrology*, 278, 197-212,  
716 [https://doi.org/10.1016/S0022-1694\(03\)00142-2](https://doi.org/10.1016/S0022-1694(03)00142-2), 2003.

717 Urban, G. and Strug, K.: Evaluation of precipitation measurements obtained from different types of rain gauges,  
718 *Meteorologische Zeitschrift*, 30, 445-463, <https://doi.org/10.1127/metz/2021/1084>, 2021.

719 [Villalobos Herrera, R., Blenkinsop, S., Guerreiro, S. B., O'Hara, T., Fowler, H. J.: Sub-hourly resolution quality control of](#)  
720 [rain gauge data significantly improves regional sub-daily return level estimates, \*Quarterly Journal of the Royal\*](#)  
721 [\*Meteorological Society\* \(submitted\), 2022.](#)

722 WMO-No. 8: Guide to Instruments and Methods of Observation, vol. I: Measurement of Meteorological Variables, 2018  
723 edition. World Meteorological Organization, Geneva, pp. 548., 2018.

724 WMO-No. 305: Guide on the Global Data-processing System, 1993 edition. World Meteorological Organization, Geneva, pp.  
725 199, 1993.

726 WMO-No. 488: Guide to the Global Observing System, 2010 edition, updated in 2017. World Meteorological Organization,  
727 Geneva, pp. 215, 2017.

728 Yeung, H.Y., Man, C., Chan S.T., and Seed, A.: Development of an operational rainfall data quality-control scheme based on  
729 radar-raingauge co-kriging analysis, *Hydrological Sciences Journal*, 59, 1293-1307,  
730 <https://doi.org/10.1080/02626667.2013.839873>, 2014.

731 You, J., Hubbard K. G., Nadarajah S., and Kunkel K. E.: Performance of quality assurance procedures on daily precipitation,  
732 *Journal of Atmospheric and Oceanic Technology*, 24, 821-834, <https://doi.org/10.1175/JTECH2002.1>, 2007.

733